The Original

# ANT LION OPTIMIZER DUAL MODE FRACTIONAL ORDER PROPORTIONAL INTEGRAL CONTROLLER FOR MULTI-AREA POWER SYSTEMS WITH RENEWABLE ENERGY SOURCES AND INTEGRATING ELECTRICAL VEHICLE CHARGING STATIONS

**Uthayabanu Nedumaran[1], Mohamed Thameem Ansari Musthafa[2]**

[1] Research Scholar, Department of Electrical Engineering, Annamalai University, Tamil Nadu, India
[2] Professor, Department of Electrical Engineering, Annamalai University, Tamil Nadu, India uthayanedumaran@gmail.com

**ABSTRACT**
The increasing penetration of renewable energy sources (RESs), electric vehicles (EVs), and rapidly varying load demands has introduced significant challenges in maintaining frequency stability in modern interconnected power systems. Conventional load frequency control (LFC) methods with fixed or inadequately optimized controller parameters often exhibit poor dynamic performance under such uncertain operating conditions. To address these challenges, this paper proposes an Ant Lion Optimizer (ALO)-based Dual-Mode Fractional-Order Proportional-Integral (DMFOPI) controller for a three-area interconnected power system incorporating RESs and EV charging stations. For a comprehensive performance evaluation, conventional Proportional-Integral (PI), Dual-Mode PI (DMPI), Fractional-Order PI (FOPI), and the proposed DMFOPI controllers are optimally tuned using the ALO algorithm based on the Integral Square Error (ISE) performance criterion.
The proposed controller is validated in the MATLAB/Simulink environment under step load disturbances, EV integration, and ±20% turbine time-constant variations. Simulation results demonstrate that the ALO-DMFOPI controller achieves superior frequency regulation with reduced frequency deviations, improved damping characteristics, shorter settling times, and enhanced disturbance rejection compared with the PI, DMPI, and FOPI controllers. The proposed controller achieves the minimum ISE value of 0.21836 and the lowest performance index (J = 0.1128), indicating its improved control effectiveness.
Furthermore, the proposed controller maintains robust and reliable performance under both EV-connected and EV-disconnected operating conditions, as well as under turbine parameter uncertainties. The results confirm that the ALO-DMFOPI controller is an effective and robust solution for load frequency control in modern interconnected power systems with high penetration of renewable energy sources and electric vehicles.

**KEYWORDS:** Ant Lion Optimizer (ALO); Load frequency control (LFC); Dual-mode fractional-order PI controller; Electric vehicles (EVs); Renewable energy sources (RESs); multi-area interconnected power system; Frequency regulation.

## INTRODUCTION
The transformation of conventional electric power systems into sustainable and intelligent energy networks has accelerated the integration of renewable energy sources (RESs) and electrified transportation. Solar photovoltaic (PV) and wind energy are increasingly deployed to reduce greenhouse gas emissions and dependence on fossil fuels. At the same time, the rapid growth of electric vehicle (EV) adoption has introduced new and highly variable electricity demand. Although these developments support environmental and energy sustainability goals, they also increase the operational complexity of interconnected power systems.
Unlike conventional thermal generation, renewable energy resources produce power that depends on weather conditions and therefore cannot always be predicted accurately. Similarly, the charging behaviour of electric vehicles varies according to user preferences, charging schedules, and traffic patterns. These uncertainties create continuous mismatches between power generation and load demand, leading to frequency fluctuations and deviations in scheduled tie-line power exchange. Consequently, maintaining frequency stability has become one of the most important operational requirements in modern interconnected power systems with significant penetration of renewable generation and EV charging infrastructure.
Load Frequency Control (LFC) is a fundamental secondary control mechanism that restores the system frequency to its nominal value following disturbances while maintaining the scheduled power transfer among interconnected control areas. A well-designed LFC strategy improves dynamic stability, enhances power quality, and ensures reliable operation during changes in generation or load demand. The effectiveness of an LFC system is influenced by the controller structure, the tuning methodology adopted for controller parameters, and the optimization objective used during the design process.

Conventional proportional-integral (PI) controllers remain widely employed because of their simple implementation and satisfactory steady-state performance. However, fixed-parameter PI controllers are often unable to provide adequate dynamic performance when the operating conditions vary significantly or when the system exhibits nonlinear behaviour. In interconnected systems containing renewable energy sources and EV charging stations, these limitations become more pronounced because of the frequent and unpredictable disturbances introduced into the network.

To overcome these shortcomings, researchers have investigated advanced control approaches, including fractional-order controllers, intelligent control methods, and optimization-based controller design. Fractional-order control provides additional tuning flexibility through non-integer integration, enabling improved transient response and robustness. Likewise, dual-mode control strategies enhance performance by employing different control actions during transient and steady-state operating conditions. Nevertheless, the overall effectiveness of these controllers depends heavily on the optimization algorithm used to determine their parameters.

Metaheuristic optimization techniques have become effective tools for solving complex controller tuning problems because they can efficiently search multidimensional solution spaces without requiring gradient information. Algorithms such as Particle Swarm Optimization (PSO), Grey Wolf Optimizer (GWO), Jaya Algorithm, Bird Swarm Algorithm (BSA), and Ant Lion Optimizer (ALO) have demonstrated promising performance in power system control applications. Among these techniques, the Ant Lion Optimizer offers an effective balance between global exploration and local exploitation, enabling rapid convergence towards high-quality solutions while reducing the possibility of premature convergence.

Although considerable progress has been reported in optimization-based load frequency control, many existing investigations focus on either conventional PI or fractional-order controllers and often consider renewable energy sources or electric vehicles individually. Studies that simultaneously address renewable generation, EV charging stations, and multi-area interconnected power systems using an optimally tuned dual-mode fractional-order controller remain comparatively limited. This research gap motivates the development of a more robust control strategy capable of maintaining satisfactory dynamic performance under a wide range of operating conditions.

To address these challenges, this work proposes an Ant Lion Optimizer (ALO)-based Dual-Mode Fractional-Order Proportional-Integral (DMFOPI) controller for load frequency control in a three-area interconnected power system integrating renewable energy sources and electric vehicle charging stations. The Ant Lion Optimizer is employed to determine the optimal controller parameters by minimizing the Integral Square Error (ISE) objective function. The proposed controller combines the rapid transient response of dual-mode control with the flexibility and robustness provided by fractional-order integration.

The performance of the proposed controller is investigated through comprehensive MATLAB/Simulink simulations under step load disturbances, electric vehicle operating conditions, and ±20% variations in turbine time constants. Its performance is compared with optimally tuned PI, Dual-Mode PI (DMPI), and Fractional-Order PI (FOPI) controllers using identical operating conditions. The obtained results demonstrate that the proposed ALO-DMFOPI controller provides improved frequency regulation, reduced oscillations, shorter settling time, enhanced disturbance rejection, and superior robustness for modern interconnected power systems with renewable energy and electric vehicle integration.

## 2. OBJECTIVES OF THE WORK

**The primary objectives of this research are summarized as follows:**

To develop a mathematical model of a three-area interconnected power system incorporating renewable energy sources (RESs), electric vehicle (EV) charging stations, and tie-line power exchanges for load frequency control (LFC) analysis. To design and optimally tune Proportional-Integral (PI), Dual-Mode Proportional-Integral (DMPI), Fractional-Order Proportional-Integral (FOPI), and the proposed Dual-Mode Fractional-Order Proportional-Integral (DMFOPI) controllers using the Ant Lion Optimizer (ALO) based on the Integral Square Error (ISE) performance criterion.

To evaluate and compare the dynamic performance of the PI, DMPI, FOPI, and DMFOPI controllers in terms of frequency deviation, peak overshoot, peak undershoot, settling time, damping characteristics, and performance index.

To investigate the effectiveness of the proposed controller under different operating scenarios, including: Step load disturbances.

System operation with and without electric vehicle (EV) integration.

To assess the robustness of the proposed controller through sensitivity analysis by introducing ±20% variations in turbine time constants and examining its ability to maintain stable system performance under parameter uncertainties.

## 3. Mathematical Modelling of the Three-Area Interconnected Power System

To assess the effectiveness of the proposed controller under realistic operating conditions, a three-area interconnected power system comprising thermal generating units, solar photovoltaic (PV) plants, electric vehicle (EV) charging stations, local loads, and tie-line interconnections is considered. The increasing penetration of renewable energy sources (RESs) and EVs introduces intermittent generation and stochastic load variations, resulting in continuous power imbalance and frequency deviations. Therefore, an accurate mathematical model is essential to investigate the dynamic behaviour of the interconnected system and evaluate the performance of

the proposed load frequency control (LFC) strategy.
The single-line representation of the investigated three-area interconnected power system is shown in Fig. 1, while the complete MATLAB/Simulink implementation of the proposed system is presented in Fig. 2.

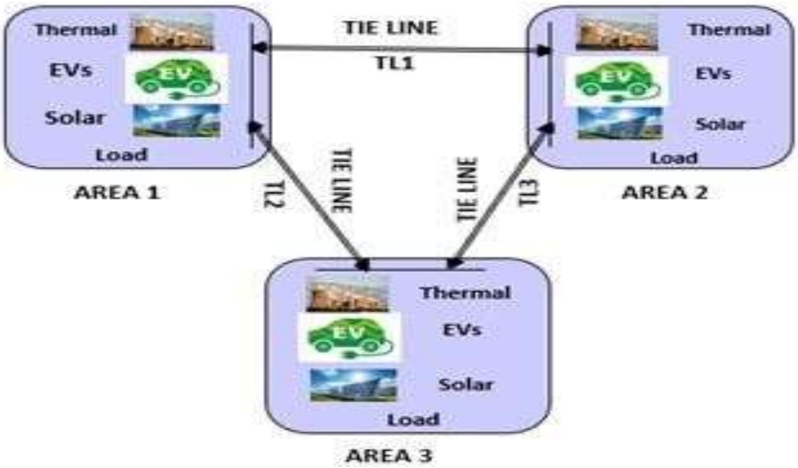


**Figure 1 Single-line diagram of the three-area interconnected power system.**

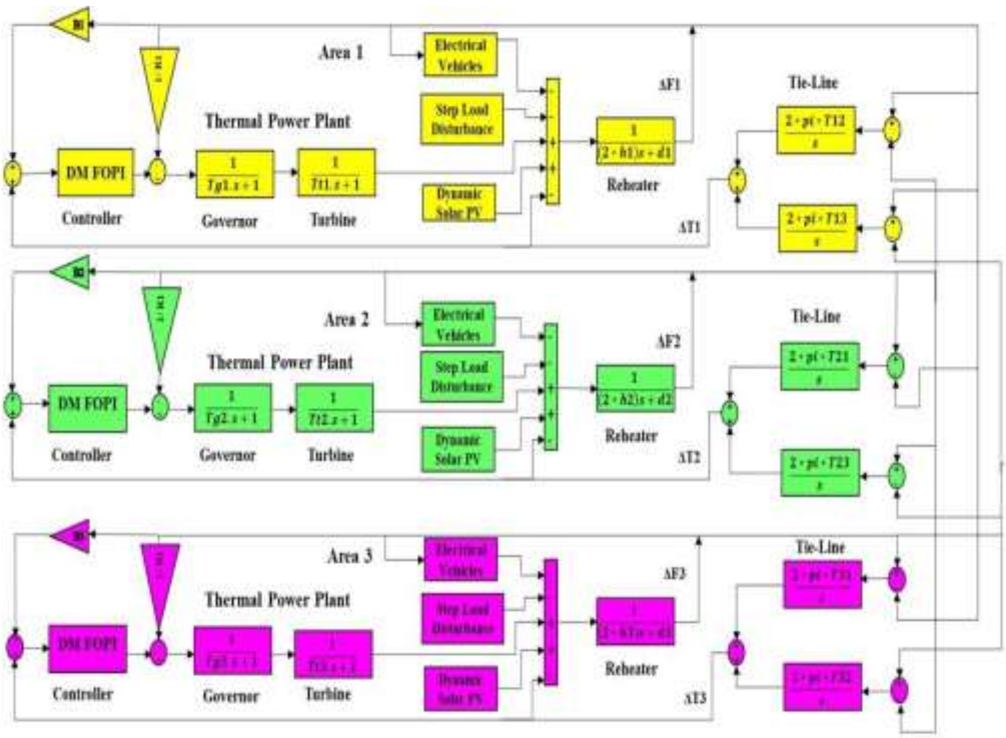


**Figure 2 MATLAB/Simulink model of the three-area interconnected power system.**

### 3.1 Mathematical Model of the Thermal Power Plant

Each control area consists of a conventional thermal generating unit equipped with a speed governor, steam turbine, and generator-load dynamics. The governor regulates the turbine input according to the frequency deviation, whereas the turbine converts the governor output into mechanical power. The generator-load dynamics represent the relationship between power imbalance and system frequency variation. Together, these subsystems determine the primary frequency response of each control area.

The transfer function of the governor is expressed as

$$G_{governor}(S) = \frac{1}{T_g.s+1} \qquad (1)$$

where

$T_g$= Governor time constant (s)

The steam turbine is represented by

$$G_{turbine}(S) = \frac{1}{T_t.s+1} \qquad (2)$$

where

$T_t$= Turbine time constant (s)

The generator-load dynamics are described by

$$G_{Reheater}(S) = \frac{1}{(2*h_1).s+1} \qquad (3)$$

where

h = Inertia constant (pu·s)

The thermal generating unit provides the primary source of power generation, while the governor and turbine cooperate to compensate for frequency deviations caused by load disturbances and renewable power fluctuations.

### 3.2 Mathematical Model of the Solar Photovoltaic System

The intermittent nature of solar irradiance introduces continuous variations in photovoltaic power generation, which significantly influence the frequency stability of interconnected power systems. To represent these fluctuations, a dynamic solar PV model is incorporated into each control area.

The stochastic behaviour of solar irradiance is simulated by injecting a white-noise signal into the PV model, thereby producing realistic power variations corresponding to changing weather conditions. The developed PV model is illustrated in Fig. 3.

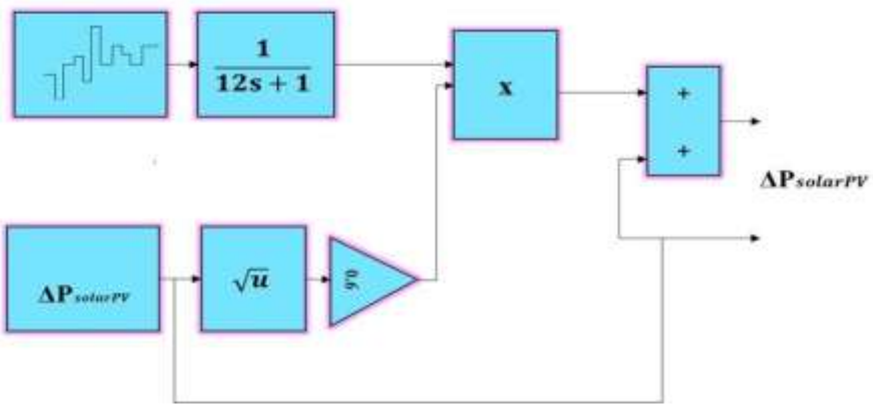


**Figure 3 Dynamic solar photovoltaic model.**

The variation in PV output power is mathematically represented as

$$\Delta P solarPV = 0.6\sqrt{P solarPV} \qquad (4)$$

where

$\Delta P solarPV$ = Variation in photovoltaic power output

$P solarPV$ = Nominal photovoltaic power

The proposed model enables realistic simulation of renewable energy uncertainty during load frequency control analysis.

### 3.3 Mathematical Model of the Electric Vehicle

Electric vehicles are modelled as distributed energy storage devices capable of either absorbing power from the grid during charging or supplying power back to the system during discharging. Consequently, EVs can actively participate in frequency regulation by rapidly responding to power imbalance conditions.

The dynamic model of the EV considered in this work is shown in Fig. 4.

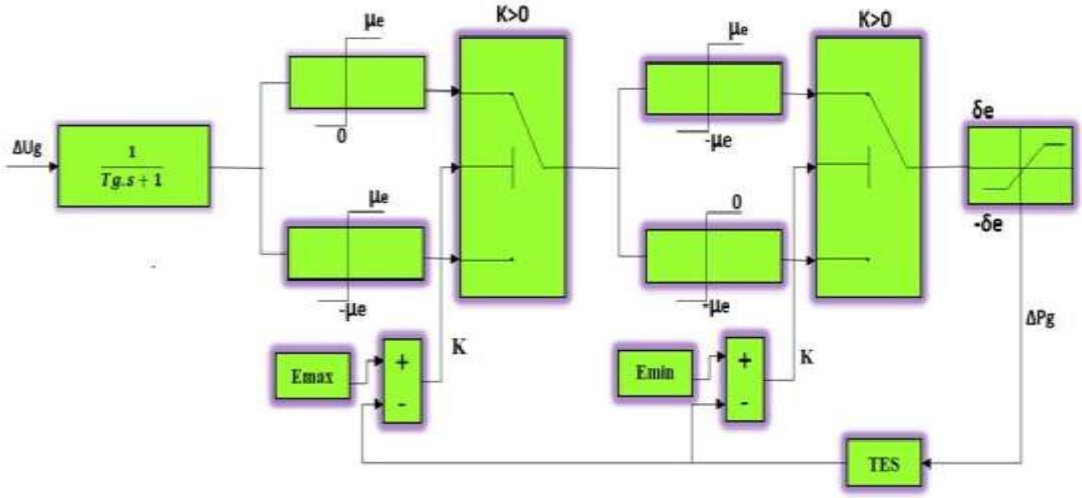


**Figure 4 Dynamic model of the electric vehicle.**

The input signal to the EV model is represented by UE , while the battery dynamics are characterized by the battery time constant TE . The inverter power rating is limited by μe , and the charging/discharging ramp-rate constraints are represented by ±δe . The battery energy is restricted within the limits Emax and Emin to ensure safe operation. The exchanged EV power is denoted by ΔPE .
ΔPE > 0: EV discharging mode ΔPE < 0: EV charging mode ΔPE = 0: Idle operating condition
When the battery reaches the upper energy limit (Emax ), further charging is prohibited and only discharging operation is permitted. Likewise, when the battery energy decreases to Emin , only charging operation is allowed. These operating constraints ensure practical implementation of EV-based frequency support under varying operating conditions.

### 3.4 Mathematical Model of the Tie-Line

The tie-line interconnects neighboring control areas and facilitates power exchange to maintain generation-load balance throughout the interconnected system. Variations in frequency between adjacent areas produce changes in tie-line power flow, making tie-line dynamics an essential component of multi-area load frequency control.
The transfer function representing the tie-line dynamics is given by

$$G_{Tie}(s) = \frac{2*pi*T_{ij}}{s} \qquad (5)$$

$T_{ij}$= Synchronizing coefficient between Areas i and j
The tie-line enables coordinated frequency regulation by allowing power transfer among interconnected areas whenever local generation and demand become unbalanced.

### 3.5 Area Control Error (ACE)

The Area Control Error (ACE) is employed as the feedback signal for the load frequency controller. It combines the local frequency deviation and tie-line power deviation to determine the corrective control action required for each control area.
The ACE for the $i^{th}$ control area is defined as
$ACE_i = B_i * \Delta f_i + \Delta P_{Tie,i}$ (6) where

$B_i$= Frequency bias constant
$\Delta f_i$= Frequency deviation of Area i
$\Delta P_{Tie,i}$ =Tie-line power deviation

The calculated ACE is supplied to the proposed DMFOPI controller, which generates the control signal required to restore system frequency and scheduled tie-line power exchange.

**Table 1 System Parameters Used in the Mathematical Model**

| Symbol | Description |
|---|---|
| $T_g$ | Governor time constant |
| $T_t$ | Turbine time constant |
| h | Inertia constant |
| B | Frequency bias constant |

| | |
|---|---|
| $T_{ij}$ | Tie-line synchronizing coefficient |
| **ΔP** $solarPV$ | Solar PV power variation |
| **ΔPE** | Electric vehicle power variation |
| $\Delta f$ | Frequency deviation |

## 4. Controller Design

This section describes the controller configurations investigated for the load frequency control (LFC) problem in the proposed three-area interconnected power system. Four controller structures are considered to evaluate the influence of different control philosophies on system performance. These include the conventional Proportional-Integral (PI) controller, the Fractional-Order Proportional-Integral (FOPI) controller, the Dual-Mode Proportional-Integral (DMPI) controller, and the proposed Dual-Mode Fractional-Order Proportional-Integral (DMFOPI) controller. For each controller, the design parameters are optimized using the Ant Lion Optimizer (ALO) to obtain improved dynamic performance under identical operating conditions.

### 4.1 Design of the ALO-Based PI Controller

The proportional-integral controller serves as the reference control strategy because of its straightforward implementation and widespread use in power system applications. The controller produces the control signal by combining a proportional action, which reacts immediately to the Area Control Error (ACE), with an integral action that gradually eliminates steady-state frequency deviations.
The control structure of the conventional PI controller is illustrated in Fig. 5.

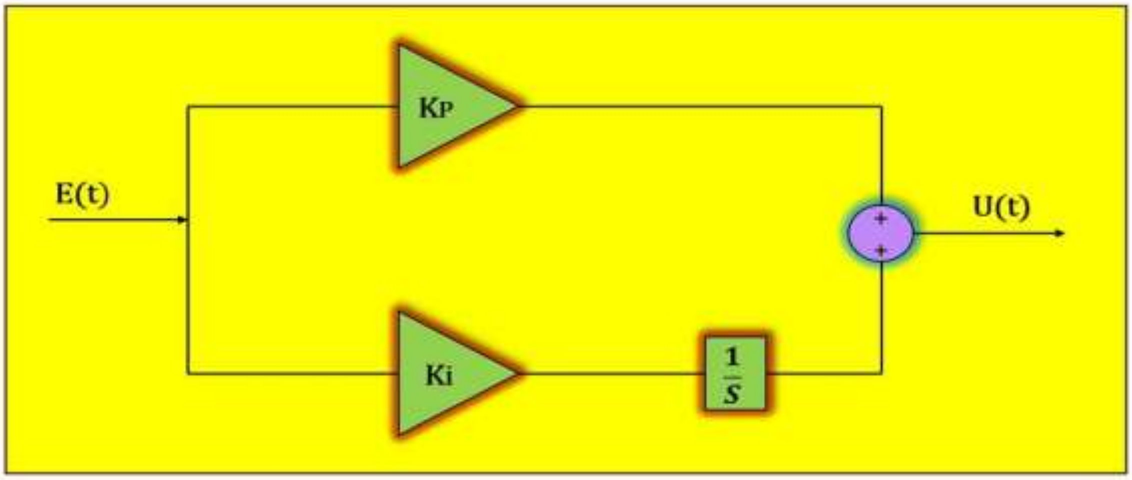


**Figure 5 Conventional PI controller.**

The controller output is expressed as

$$U(t)=\boldsymbol{K_p}E(t)+\int_0^t \frac{k_i}{s} E(t) \qquad (7)$$

where
U(t)= denotes the control signal,
E(t)= represents the Area Control Error (ACE),
$K_p$ = is the proportional gain,
$K_i$ = is the integral gain.
Although the PI controller provides satisfactory steady-state accuracy, its dynamic performance deteriorates under parameter uncertainties, renewable energy fluctuations, and large load disturbances. Therefore, advanced controller structures are required for modern interconnected power systems.

### 4.2 Design of the ALO-Based Fractional-Order PI Controller

To improve control flexibility, the conventional integral term is replaced by a fractional-order integrator. This modification introduces an additional tuning parameter that allows the controller to better accommodate nonlinear and time-varying system behaviour.

The structure of the FOPI controller is presented in Fig. 6.

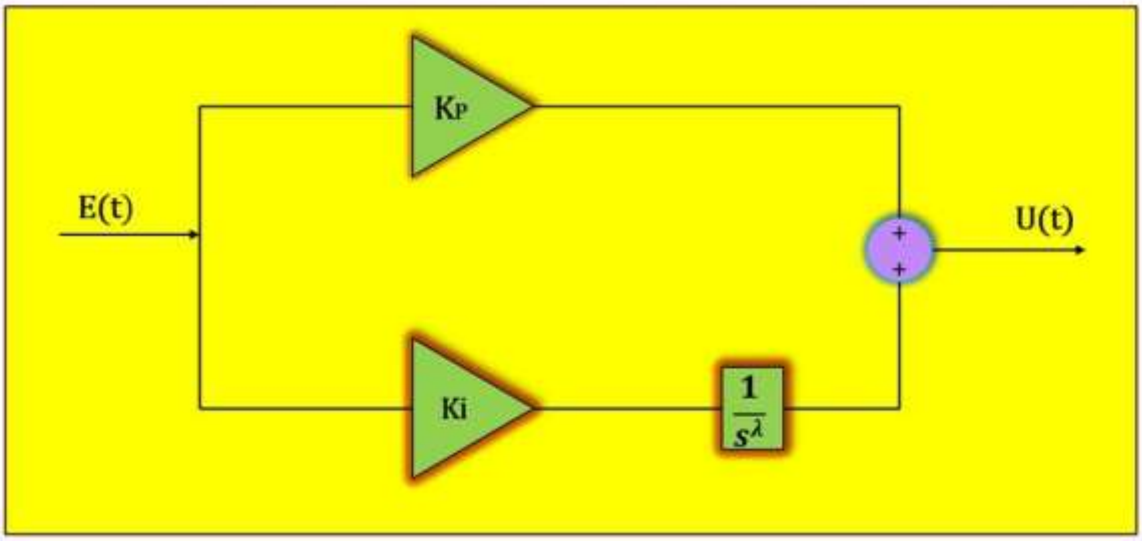


**Figure 6 Conventional fractional-order PI controller.**

$$U(t)= \boldsymbol{K_p}\ E(t)+\int_{0}^{t} \frac{k_i}{s^{\lambda}}\, E(t) \qquad (8)$$

where

$\lambda$ = is the fractional integration order, $0<\lambda<1$.

When

$\lambda=1$

the FOPI controller reduces to the conventional PI controller. The additional tuning parameter allows improved controller adaptability under nonlinear and time-varying operating conditions.

### 4.3 Design of the ALO-Based Dual-Mode PI Controller

The Dual-Mode PI controller introduces a switching mechanism that changes the control action according to the magnitude of the Area Control Error. Instead of continuously applying proportional and integral actions simultaneously, the controller activates the most appropriate operating mode for the prevailing system condition. The switching logic is illustrated in Fig. 7.

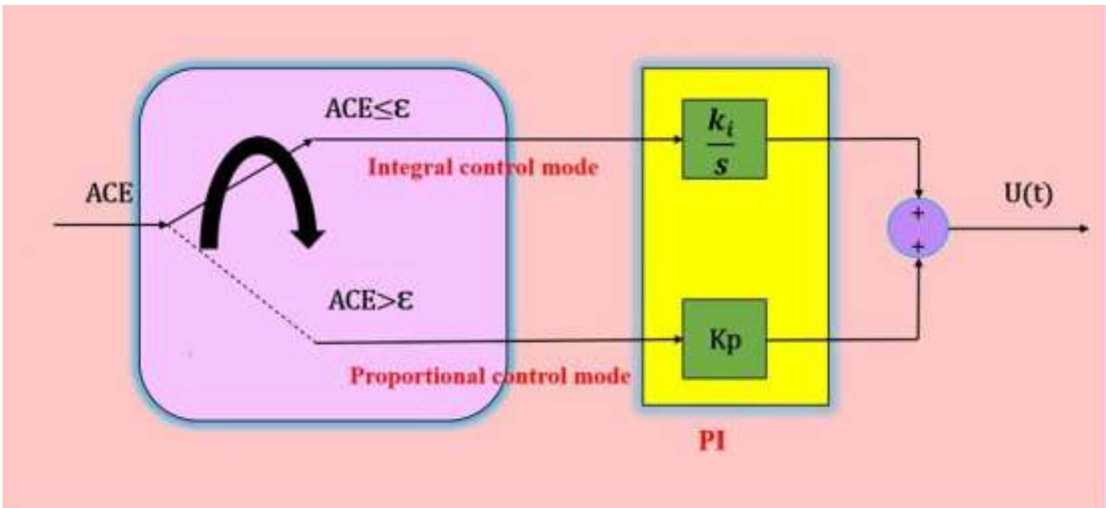


**Figure 7 Dual-mode PI controller.**

A positive threshold value ε determines the operating mode. When
$|e(t)| > \varepsilon$
the proportional mode is activated to provide a rapid response during large disturbances. When
$|e(t)| \leq \varepsilon$
the controller switches to integral mode to eliminate steady-state frequency error.
This switching strategy reduces unnecessary control action while improving settling characteristics and frequency regulation.

### 4.4 Design of the Proposed ALO-Based DMFOPI Controller

To further improve the frequency regulation capability of the interconnected system, a Dual-Mode Fractional-Order Proportional-Integral controller is proposed. The controller combines the rapid switching characteristics of dual-mode control with the enhanced flexibility provided by fractional-order integration. The controller structure is shown in Fig. 8.

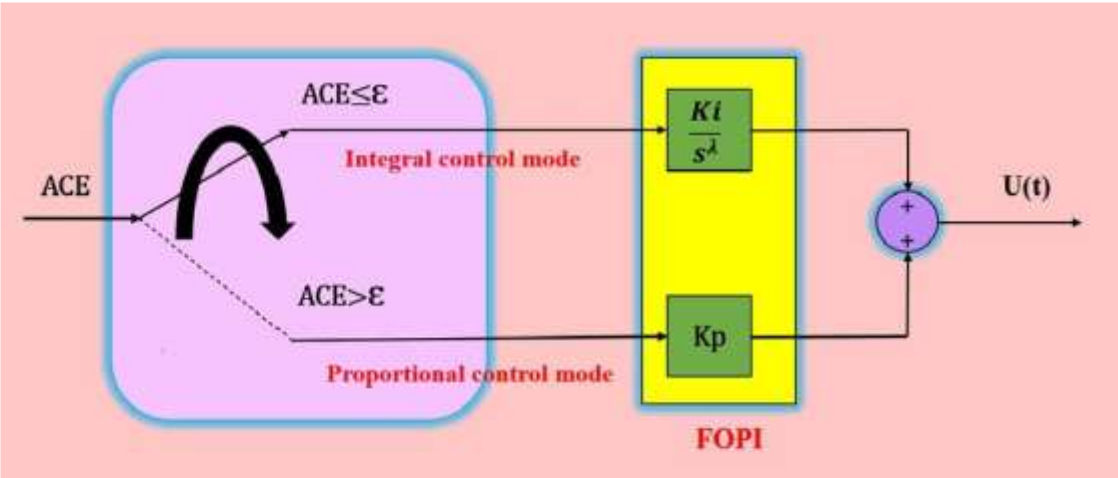


**Figure 8 Proposed dual-mode fractional-order PI controller.**

The controller continuously monitors the Area Control Error and selects the appropriate operating mode according to the predefined switching threshold. During large disturbances, proportional control produces an immediate corrective action that accelerates frequency recovery. As the error decreases, the controller changes to fractional-order integral control, which gradually removes the remaining error while improving damping characteristics.
The switching rules are defined as $U(t) = K_P e(t), |e(t)| > \varepsilon$ (9)

$U(t) = \frac{K_i}{s} e(t), |e(t)| \leq \boldsymbol{\varepsilon}$ (10)

For the proposed DMFOPI controller,

$U(t) = \frac{K_i}{s^\lambda} e(t), |e(t)| \leq \boldsymbol{\varepsilon}$ (11)

where
$K_P$ = proportional gain,
$K_i$= integral gain,
$\lambda$ = fractional-order parameter,
$\varepsilon$ = switching threshold.
The value of $\lambda$ is selected within the interval 0 < < 1
When
$\lambda$ =1
the proposed controller becomes identical to the Dual-Mode PI controller.
By combining adaptive mode switching with fractional-order integration, the proposed controller is capable of improving transient performance, reducing oscillatory behaviour, enhancing disturbance rejection, and maintaining satisfactory operation under renewable energy fluctuations, electric vehicle integration, and parameter variations.

**Table 2 Comparison of PI, DMPI, FOPI, and DMFOPI Controllers**

| Controller Type | Structure | Tunable Parameters | Key Features | Limitations |
|---|---|---|---|---|
| **PI** | Proportional + Integral | $K_P$, $K_i$ | Simple design, eliminates steady-state error | Limited robustness, poor performance under large disturbances or nonlinearities |

| | | | | |
|---|---|---|---|---|
| **Dual PI** | Dual mode PI controllers | $K_P$, $K_i$, ε | Improved transient response and stability | More complex tuning, can lead to interaction issues between loops |
| **FOPI** | Proportional + Fractional Integral (order λ) | $K_P$, $K_i$, λ | Better robustness and disturbance rejection | Fractional calculus implementation complexity, tuning is more difficult |
| **Dual FOPI** | Dual mode FOPI controllers | $K_P$, $K_i$, ε, λ | Combines dual-loop benefits with fractional-order control | Highest complexity, challenging tuning and implementation, computationally intensive |

Table 2 compares the characteristics of the PI, DMPI, FOPI, and DMFOPI controllers in terms of controller structure, tunable parameters, advantages, and implementation complexity. Among the investigated methods, the proposed DMFOPI controller provides the greatest design flexibility because it incorporates both the switching threshold and the fractional-order parameter. Although additional optimization variables are required, this increased flexibility enables superior dynamic performance and improved robustness over a wide range of operating conditions.

**Table 3 Tunable Parameters of the Controllers**

| **Parameters** | **ALO-PI** | **ALO-DMPI** | **ALO-FOPI** | **ALO-DMFOPI** |
|---|---|---|---|---|
| $K_P$ | ✓ | ✓ | ✓ | ✓ |
| $K_i$ | ✓ | ✓ | ✓ | ✓ |
| $\boldsymbol{\lambda}$ | | | ✓ | ✓ |
| $\boldsymbol{\varepsilon}$ | | ✓ | | ✓ |

Similarly, Table 3 summarizes the optimization parameters considered for each controller. The PI controller requires optimization of only the proportional and integral gains, whereas the FOPI controller additionally includes the fractional-order parameter. The DMPI controller introduces the switching threshold, while the proposed DMFOPI controller simultaneously optimizes the proportional gain, integral gain, fractional-order parameter, and switching threshold. This comprehensive parameter optimization contributes to the improved control performance observed in the simulation studies.

## 5. Problem Formulation and Ant Lion Optimizer (ALO)

This section presents the optimization framework adopted to determine the controller parameters for the investigated load frequency control (LFC) problem. The optimization process aims to identify the parameter combination that provides the best dynamic response by minimizing the selected performance criterion.

The Ant Lion Optimizer (ALO) is employed as the search algorithm because of its ability to explore the solution space effectively while progressively refining promising solutions.

### 5.1 Problem Formulation

The controller design is formulated as an optimization problem in which the objective is to minimise the frequency deviations produced by disturbances in the interconnected power system. To evaluate the quality of each solution, the Integral Square Error (ISE) is selected as the objective function since it penalizes large deviations more severely and encourages rapid system stabilization.

The Area Control Error (ACE) for each control area is expressed as

$$ACE_i = \Delta P_{tie,ij} + \beta_i \Delta F_i \qquad (12)$$

where

$\Delta P_{tie,ij}$ = Denotes the tie-line power deviation between the $i^{th}$ and $j^{th}$ control areas,

$\Delta F_i$ = Represents the frequency deviation of the $i^{th}$ area,

$\beta_i$= is the frequency bias coefficient.

The optimization objective is to minimize the Integral Square Error (ISE), defined as

$$J = \int_0^t (ACE(t))^2 dt \qquad (13)$$

The optimization process is performed subject to the following constraints on the controller parameters:

$$K_{p,min} \le K_p \le K_{p,max}$$

$K_{i,min} \leq K_i \leq K_{i,max}$
$\lambda_{min} \leq \lambda \leq \lambda_{max}$
$\varepsilon_{min} \leq \varepsilon \leq \varepsilon_{max}$

where $K_p$ and $K_i$ are the proportional and integral gains, respectively, $\lambda$ denotes the fractional-order parameter, and
represents the switching threshold used in the dual-mode controllers.

The Ant Lion Optimizer is employed to obtain the optimal controller parameters that minimize the objective function while satisfying the above constraints. The optimization is carried out individually for the PI, DMPI, FOPI, and proposed DMFOPI controllers.

### 5.2 Ant Lion Optimizer (ALO)

The Ant Lion Optimizer is a population-based optimization technique that imitates the hunting strategy of antlion larvae. Instead of relying on gradient information, the algorithm searches for improved solutions by repeatedly updating the positions of solutions through a combination of exploration and exploitation mechanisms.

In this study, controller parameter set is represented as an ant, whereas antlions correspond to promising regions within the search space. Throughout the optimization process, move within the feasible region while being influenced by both selected antlions and the best solution identified during previous iterations. This search strategy enables the algorithm to investigate different regions initially and progressively concentrate on high-quality solutions as convergence proceeds. The optimization continues until the specified termination criterion is satisfied, after which the parameter set producing the minimum objective function value is selected for controller implementation.

### 5.3 Mathematical Modelling of ALO

The mathematical formulation of the ALO algorithm begins with the random generation of ant and antlion populations inside the permissible search limits. The objective value is evaluated by executing the LFC simulation model.

During each iteration, the ALO algorithm executes three sequential stages: (i) Random Walk of Ants, (ii) Trap Formation by Antlions, and (iii) Elite Effect. Together, these stages balance global exploration and local exploitation, enabling the algorithm to efficiently search for the optimal controller parameters.

The flowchart of the proposed optimization methodology is presented in Fig. 9, while the ALO control parameters used in this study are summarized in Table 4.

**Table 4 ALO control parameters**

| ALO Parameters | Value |
|---|---|
| Number of ant lion | 30 |
| Maximum iteration | 50 |
| Learning Factor | 2 |
| Lower bound limit | -1 |
| Upper bound limit | 1 |

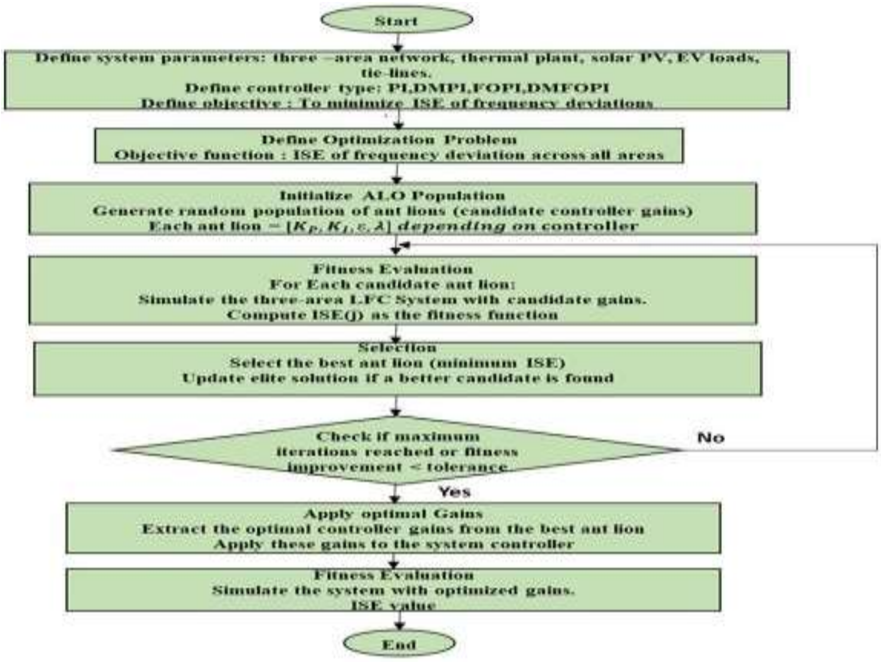


**Figure 9 flowchart of the proposed optimization methodology Pseudocode of the ALO-Based Optimization**

1. Define the optimization variables and their permissible limits.
2. Generate the initial populations of ants and antlions randomly.
3. Evaluate the objective function for every solution.
4. Identify the current best solution (elite).
5. Repeat until the stopping criterion is satisfied:

Generate new solutions through stochastic movement. Evaluate the objective function.

Update antlion positions whenever an improved solution is obtained. Replace the elite solution if a better objective value is found.

6. Return the controller parameters corresponding to the minimum ISE value.

## 6. RESULTS AND DISCUSSION

This section presents the simulation results obtained for the proposed load frequency control (LFC) strategy in a three-area interconnected power system integrated with renewable energy sources and electric vehicle (EV) charging stations. The controller parameters were optimized using the Ant Lion Optimizer (ALO) by minimizing the Integral Square Error (ISE) objective function. All simulations were carried out in MATLAB/Simulink under identical operating conditions to ensure a fair comparison among the ALO-PI, ALO-DMPI, ALO-FOPI, and proposed ALO-DMFOPI controllers.

**Table 5: ALO-optimized gain values for all four controllers**

| GAIN VALUES | ALO-PI | ALO-DMPI | ALO-FOPI | ALO-DMFOPI |
|---|---|---|---|---|
| $K_{p1}$ | 0.005216 | 0.19127 | 0.95634 | 0.24354 |
| $K_{p2}$ | 0.2875 | 0.11619 | 0.026378 | 0.34651 |
| $K_{p3}$ | 0.243 | 0.52283 | 0.77669 | 0.83632 |
| $K_{i1}$ | 0.6872 | 0.98433 | 0.67582 | 0.40891 |
| $K_{i2}$ | 0.41505 | 0.70806 | 0.51425 | 0.4496 |
| $K_{i3}$ | 0.5017 | 1 | 0.28443 | 0.9255 |
| $\boldsymbol{\lambda_1}$ | - | - | 0.126 | 0.12298 |
| $\boldsymbol{\lambda_2}$ | - | - | 0.17294 | 0.35224 |
| $\boldsymbol{\lambda_3}$ | - | - | 0.9 | 0.62126 |
| $\boldsymbol{\varepsilon_1}$ | - | 0.50613 | - | 0.87263 |
| $\boldsymbol{\varepsilon_2}$ | - | 0.86551 | - | 0.73852 |
| $\boldsymbol{\varepsilon_3}$ | - | 0.14318 | - | 0.88125 |

The optimized controller gains obtained using the ALO algorithm are listed in Table 5. Since each controller has a different mathematical structure, the optimized proportional, integral, fractional-order, and dual-mode parameters vary accordingly. The optimized parameter set is subsequently used for all performance evaluations presented in this section.

**Table 6. Performance Indices Obtained for Different Controllers**

| Controller Type | ALO-PI | ALO-DMPI | ALO-FOPI | ALO-DMFOPI |
|---|---|---|---|---|
| **ISE** | 0.6631 | 0.34045 | 0.27221 | **0.21836** |

The effectiveness of the optimized controllers is first evaluated using the Integral Square Error (ISE), as summarized in Table 6. The proposed ALO-DMFOPI controller achieves the minimum ISE value of 0.21836, whereas the ALO-FOPI, ALO-DMPI, and ALO-PI controllers obtain ISE values of 0.27221, 0.34045, and 0.66310, respectively. Compared with the conventional ALO-PI controller, the proposed controller reduces the ISE by approximately 67%, while improvements of about 36% and 20% are obtained compared with the ALO-DMPI and ALO-FOPI controllers, respectively. The significant reduction in ISE demonstrates the ability of the proposed controller to suppress frequency oscillations more effectively and improve the overall dynamic performance of the interconnected power system.

**Table 7: Evaluation of Controller Performance Using Frequency Deviation, Tie-Line Power Variation, and Performance Index (J)**

| Controller Type | ALO-PI | ALO-DMPI | ALO-FOPI | ALO-DMFOPI |
|---|---|---|---|---|
| $\Delta F_1$ in Hz | 0.5261 | 0.2083 | 0.1034 | **0.04492** |

| | | | | |
|---|---|---|---|---|
| $\Delta F_2$ in Hz | 0.3650 | 0.2031 | 0.07314 | **0.03645** |
| $\Delta F_3$ in Hz | 0.4746 | 0.2088 | 0.06907 | **0.01068** |
| $\Delta T_1$ in MW | 0.5531 | 0.004562 | 0.5447 | **0.5409** |
| $\Delta T_2$ in MW | -0.6026 | -0.005962 | 0.07314 | **0.03645** |
| $\Delta T_3$ in MW | 0.04952 | 0.0014 | 0.06907 | **0.01068** |
| **Performance Index (J)** | 2.534 | 1.277 | 0.3831 | **0.1128** |

A detailed comparison of the frequency deviations, tie-line power deviations, and performance index is presented in Table 7. The conventional ALO-PI controller exhibits the largest frequency deviations in all three areas together with the highest performance index (J = 2.534), indicating relatively poor disturbance rejection capability. The ALO-DMPI controller considerably improves the transient response by reducing both the frequency deviations and tie-line power oscillations. The ALO-FOPI controller further enhances the system performance because the fractional-order control action provides greater flexibility during controller tuning. Nevertheless, the proposed ALO-DMFOPI controller consistently produces the smallest frequency deviations in all three control areas ($\Delta_1$ = 0.04492 Hz, $\Delta_2$= 0.03645 Hz, and $\Delta_3$ = 0.01068 Hz) while achieving the minimum performance index (J = 0.1128). These results confirm that the combined dual-mode and fractional-order control strategy significantly enhances disturbance rejection and frequency regulation performance.

**Table 8. Time-Domain Performance Comparison of PI, Dual-PI, FOPI, and DMFOPI Controllers**

| **Variation in Areas** | **Controller Type** | **Undershoot in percentage** | **Overshoot in percentage** | **Settling time in sec** |
|---|---|---|---|---|
| $\Delta \boldsymbol{F_1}$ **in Hz** | **ALO-PI** | 18 | 8 | 10 |
| | **ALO-DMPI** | 12 | 5 | 7 |
| | **ALO-FOPI** | 10 | 4 | 6 |
| | **ALO-DMFOPI** | 8 | 3 | 4 |
| $\Delta \boldsymbol{F_2}$ **in Hz** | **ALO-PI** | 19 | 6 | 11 |
| | **ALO-DMPI** | 11 | 5 | 8 |
| | **ALO-FOPI** | 12 | 3 | 6 |
| | **ALO-DMFOPI** | 8 | 3 | 5 |
| $\Delta \boldsymbol{F_3}$ **in Hz** | **ALO-PI** | 18 | 6 | 11 |
| | **ALO-DMPI** | 11 | 5 | 7 |
| | **ALO-FOPI** | 10 | 6 | 6 |
| | **ALO-DMFOPI** | 8 | 3 | 4 |

The transient response characteristics obtained from the simulations are summarized in Table 8. It is evident that the proposed ALO-DMFOPI controller provides the lowest undershoot, minimum overshoot, and shortest settling time among all the investigated controllers. For Area 1, the settling time is reduced from 10 s for the ALO-PI controller to 4 s using the proposed controller. Similar improvements are observed in Areas 2 and 3, where the settling time decreases from 11 s to 5 s and 4 s, respectively. Furthermore, the proposed controller limits the overshoot to approximately 3% in all three areas, whereas the conventional PI controller exhibits overshoots between 6% and 8%. These improvements indicate that the proposed controller provides faster stabilization with significantly improved damping characteristics.

To comprehensively evaluate the controller performance, three simulation scenarios are considered:

1. Performance under a step load disturbance.
2. Performance with and without EV integration.
3. Sensitivity analysis under ±20% turbine time-constant variations.

The obtained results demonstrate the effectiveness and robustness of the proposed ALO-DMFOPI controller under both nominal and disturbed operating conditions.

### 6.1 Case 1: Step Load Disturbance

A 0.2 p.u. step load disturbance is applied simultaneously to evaluate the dynamic performance of the optimized controllers. The corresponding frequency responses of Areas 1, 2, and 3 are presented in Figs. 10–12.

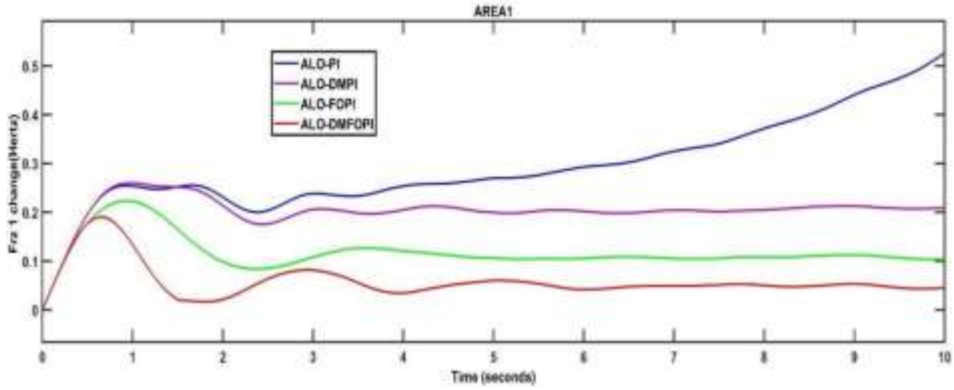


**Figure 10: Frequency deviation of Area 1**

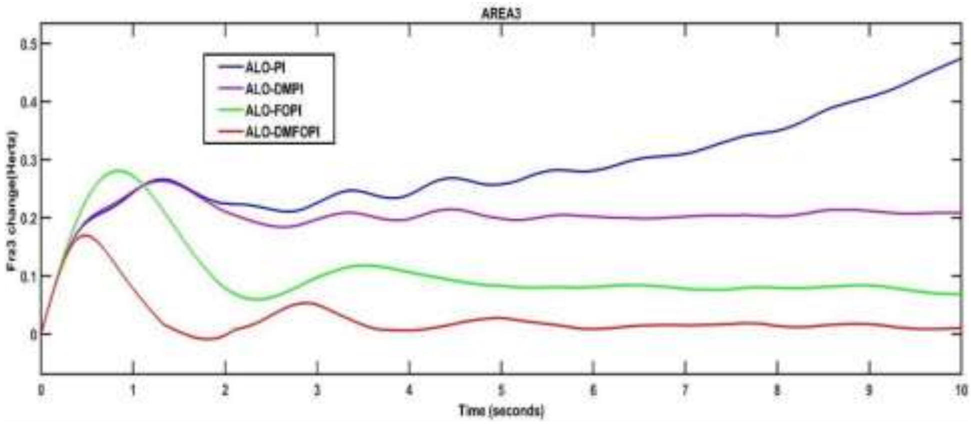


**Figure 11: Frequency deviation of Area 2**

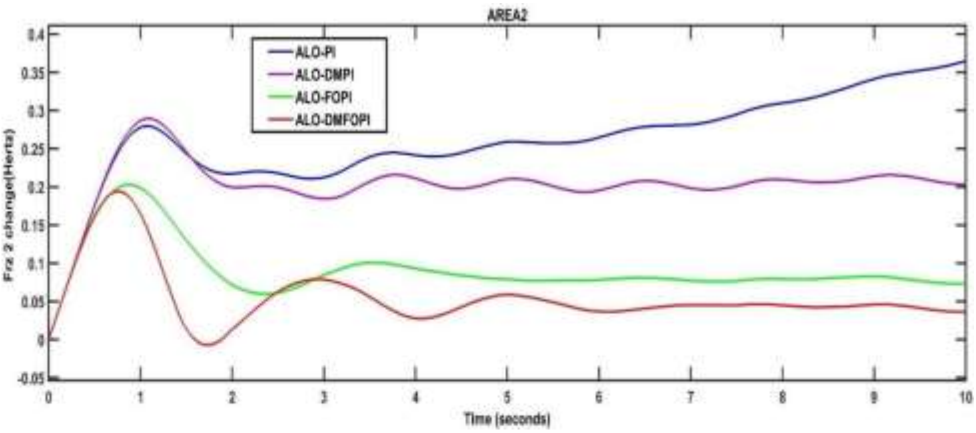


**Figure 12: Frequency deviation of Area 3**

As illustrated in Fig. 10, the conventional ALO-PI controller exhibits the largest frequency deviation together with continuously increasing oscillations, indicating inadequate damping capability and poor transient performance. Although the ALO-DMPI controller reduces the oscillation magnitude and restores the system frequency within approximately 7 s, noticeable oscillations remain during the transient period.

The ALO-FOPI controller further improves the dynamic response by utilizing fractional-order control, resulting in lower overshoot and a settling time of approximately 6 s. However, the proposed ALO-DMFOPI controller exhibits the best performance, with the smallest peak frequency deviation and a settling time of approximately 4 s. The dual-mode switching mechanism enables rapid corrective action immediately after the disturbance, while

the fractional-order control improves damping and enhances steady-state accuracy.
A similar performance trend is observed in Figs. 11 and 12 for Areas 2 and 3. In all control areas, the proposed controller effectively suppresses oscillations, minimizes frequency deviations, and restores the nominal operating frequency more rapidly than the other controllers. The improved performance demonstrates the superior capability of the proposed controller to maintain frequency stability following sudden load disturbances.

**6.2 Case 2: Performance with and without EV Integration**

The robustness of the proposed controller is further investigated by comparing the system performance with and without electric vehicle (EV) charging loads. The corresponding frequency response of Area 1 is presented in Fig. 13.

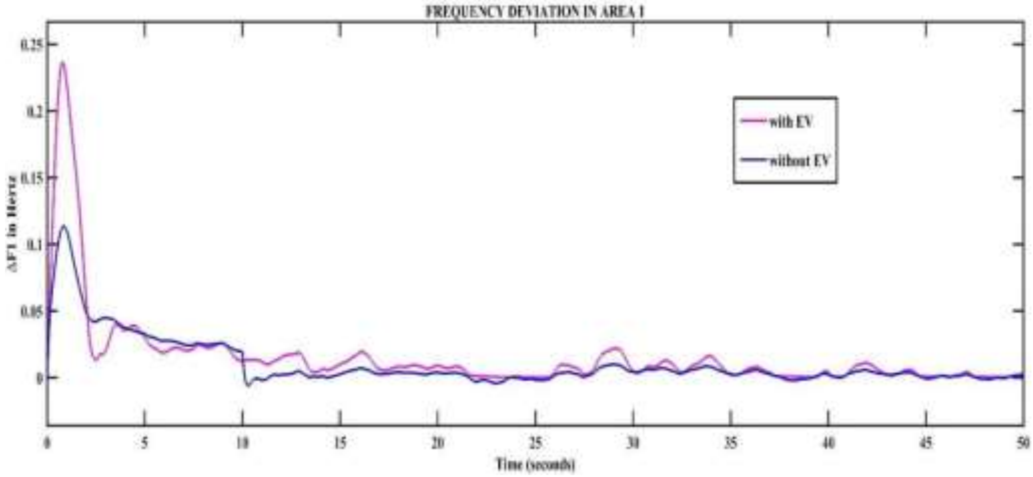


**Figure 13: Performance Analysis output obtained for Area 1**

Without EV integration, the system exhibits a relatively small initial frequency deviation and rapidly converges to the steady-state operating point with minimal oscillations. When EV charging loads are incorporated into the system, the additional and continuously varying power demand increases the initial frequency deviation and produces larger transient oscillations during the first few seconds.
Although the peak frequency deviation increases from approximately 0.10 Hz to 0.23 Hz after EV integration, the proposed ALO-DMFOPI controller successfully suppresses the oscillations and restores the system frequency to its nominal value within nearly the same settling time. In both operating conditions, the steady-state frequency deviation approaches zero after approximately 10 s, confirming the controller's capability to maintain stable system operation despite the uncertainties introduced by EV charging loads.
These results demonstrate that the proposed controller possesses excellent robustness and is well suited for modern interconnected power systems with high penetration of electric vehicles.

**6.3 Case 3: Sensitivity Analysis under Parameter Variations**

To evaluate the robustness of the proposed controller against system parameter uncertainties, a sensitivity analysis is carried out by varying the turbine time constants ($Tt_1$, $Tt_2$, and $Tt_3$) by ±20% from their nominal values.
The frequency responses corresponding to the nominal, +20%, and −20% parameter variations are presented in Figs. 14–16, while the resulting frequency deviations are summarized in Table 9.

| **Parameter** | **Change in frequency deviation** | | |
|---|---|---|---|
| | **Area 1** | **Area 2** | **Area 3** |
| **With nominal values of Tt1, Tt2, Tt3** | 0.01289 | 0.004108 | 0.03381 |
| **+20% of variation in Tt1, Tt2, Tt3** | 0.02056 | 0.009713 | 0.02892 |
| **-20% of variation in Tt1, Tt2, Tt3** | 0.01331 | 0.005914 | 0.03796 |

**Table 9: Frequency Deviation in Three Areas Under ±20% Turbine Time-Constant Variation**

The simulation results indicate that the responses obtained under the nominal and −20% parameter variations are nearly identical, exhibiting fast settling characteristics with only minor frequency deviations. Under the +20% variation, the transient response becomes comparatively slower, producing a slightly larger oscillation before converging to the steady-state condition. Nevertheless, the proposed controller maintains system stability under all operating conditions.

As shown in Table 9, the frequency deviations remain very small even after parameter variations. For example, the maximum frequency deviation in Area 1 changes only from 0.01289 Hz under nominal conditions to 0.02056 Hz under the +20% variation, demonstrating only a marginal performance degradation. Similar behaviour is observed in Areas 2 and 3, confirming that the proposed controller is insensitive to moderate variations in turbine dynamics.

Overall, the sensitivity analysis verifies that the proposed ALO-DMFOPI controller possesses excellent robustness against parameter uncertainties and can maintain satisfactory dynamic performance under practical operating conditions.

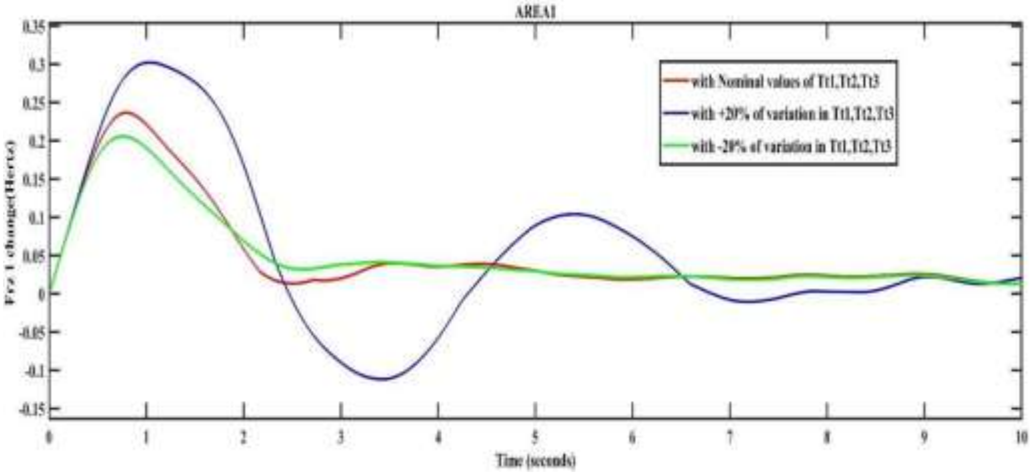


**Figure 14: Sensitivity Analysis output obtained for Area 1**

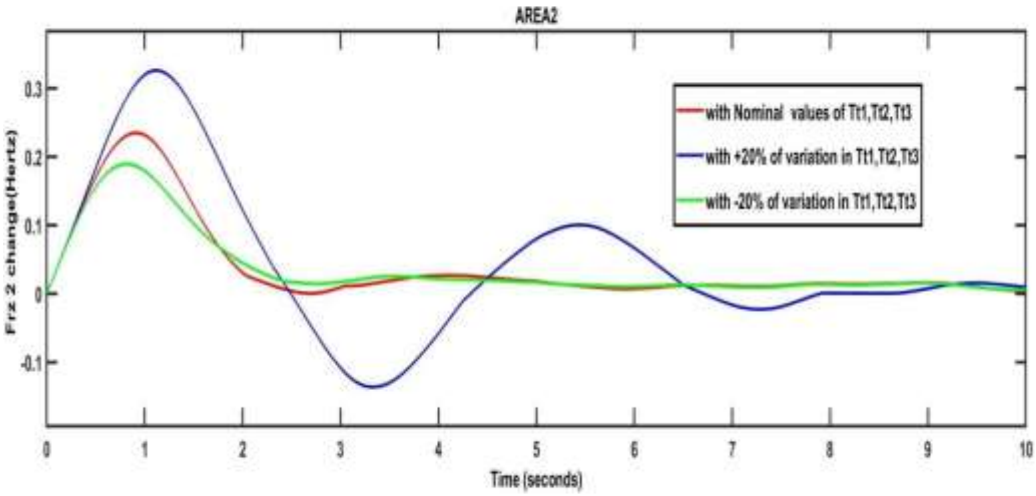


**Figure 15: Sensitivity Analysis output obtained for Area 2**

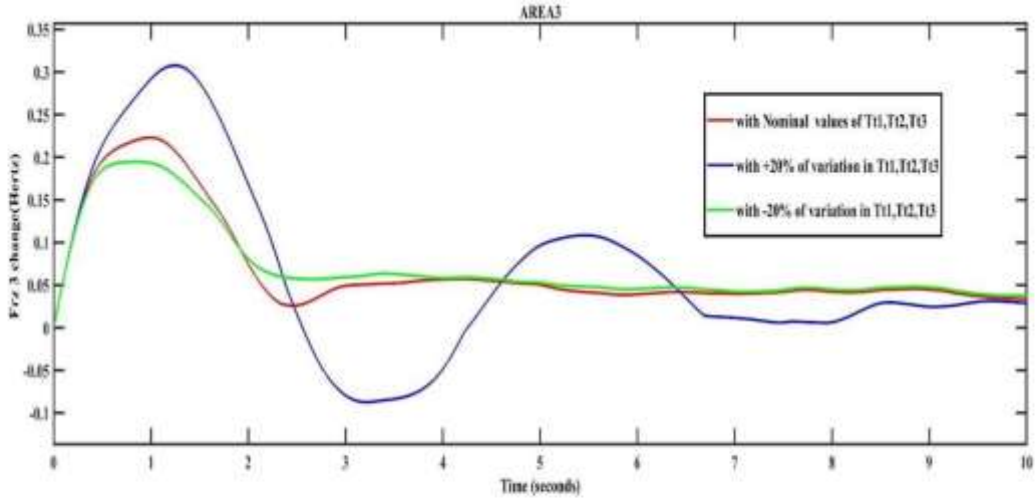


**Figure 16: Sensitivity Analysis output obtained for Area 3**

## 7. CONCLUSION AND FUTURE SCOPE

This study presented an Ant Lion Optimizer (ALO)-based Dual-Mode Fractional-Order Proportional-Integral (DMFOPI) controller for load frequency control (LFC) of a three-area interconnected power system incorporating renewable energy sources (RESs) and electric vehicle (EV) charging stations. The controller parameters were optimally tuned using the ALO algorithm by minimizing the Integral Square Error (ISE) objective function. The effectiveness of the proposed controller was evaluated in MATLAB/Simulink and compared with the ALO-optimized PI, DMPI, and FOPI controllers under identical operating conditions.

The simulation results demonstrated that the proposed ALO-DMFOPI controller consistently outperformed the existing controllers in terms of frequency regulation, disturbance rejection capability, damping characteristics, overshoot reduction, and settling time. The proposed controller achieved the minimum ISE value of 0.21836 and the lowest performance index of J=0.1128, indicating superior dynamic performance and improved system stability. Furthermore, the controller significantly reduced frequency deviations and tie-line power oscillations in all three control areas, enabling faster recovery following sudden load disturbances.

The robustness of the proposed controller was further verified through EV integration and sensitivity analysis under

±20% variations in turbine time constants. In all investigated operating conditions, the controller maintained stable system operation with minimal performance degradation, demonstrating its capability to accommodate parameter uncertainties and additional load variations introduced by EV charging. These results confirm that the proposed ALO-DMFOPI controller provides reliable and efficient frequency regulation for modern interconnected power systems with high renewable energy penetration.

Overall, the proposed optimization framework combines the global search capability of the Ant Lion Optimizer with the improved dynamic characteristics of the dual-mode fractional-order controller, resulting in enhanced transient and steady-state performance. Therefore, the proposed controller represents a promising solution for future smart grid applications requiring high reliability, robustness, and fast dynamic response.

**Appendix A**

Thermal power system Sbase = 100MW

Area 1: R1 = 3 Hz/s; Tg1= 0.08 s; Tt1= 0.4 s; D1 = 0.0084 pu/Hz; H1= 0.1677/2 pu s; T12= 0.20 pu/Hz; T13 = 0.25 pu/Hz

Area 2: R2 = 2.73 Hz/s; Tg2= 0.06 s; Tt2= 0.44 s; D2= 0.016 pu/Hz; H2= 0.2017/2 pu s; T21 = 0.20 pu/Hz: T23 = 0.12pu/Hz

Area 3: R3= 2.82 Hz/s; Tg3 = 0.07 s; Tt3= 0.30 s; D3 = 0.015 pu/Hz; H3= 0.1247/2 pu s; T31 = 0.25 pu/Hz: T32 = 0.12 pu/Hz

**REFERENCES**

1. H. Bevrani, T. Hiyama, and G. Shokoohi, “Intelligent frequency control in modern power systems: A review,” IEEE Transactions on Smart Grid, vol. 3, no. 4, pp. 2131–2141, 2012.
2. D. Sharma, “Load Frequency Control: A Literature Review”, International Journal of Scientific & Technology Research, Vol. 9, pp.6421-6437, 2020.
3. P. Kundur and N. J. Balu, “Power system frequency response and control,” IEEE Transactions on Power

Systems, vol. 36, no. 5, pp. 4217–4234, 2021.
4. B. Vedik, R. Kumar, R. Deshmukh, S. Verma, and C. K. Shiva, “Renewable Energy-Based Load Frequency Stabilization of Interconnected Power Systems Using Quasi-Oppositional Dragonfly Algorithm”, Journal of Control, Automation and Electrical Systems, vol. 32, No. 1, pp. 227-243, 2021.
5. S.S. Pati, A. Behera and T.K. Panigrahi, “ Automatic generation control of renewable energy based multi-area system with plug in electric vehicle”, International Journal of Renewable Energy Research (IJRER), Vol.10, No. 1,
pp. 54-66, March 2020.
6. A. Dorsman and M. A. Abido, “Model predictive-based PI controllers for frequency regulation in multi-area systems with renewables,” IEEE Access, vol. 8, pp. 224891–224903, 2020.
7. R. K. Jena and S. Panda, “Load frequency control of a multi-area system using fractional-order control,” in Proc. IEEE International Conference on Energy (ENVICON), pp. 241–246, 2019.
8. A. Ghosh, K. Ray, M. Nurujjaman, and M. Jamshidi, “ Voltage and frequency control in conventional and PV integrated power systems by a particle swarm optimized Ziegler – Nichols based PID controller, ” SN Applied Sciences,Vol. 3,No. 3, pp. 1-13, March 2021.
9. A. Bidram and A. Davoudi, “Hierarchical structure of microgrids control system,” IEEE Transactions on Smart Grid, vol. 3, no. 4, pp. 1963–1976, 2012.
10. Srivishnupriya Arumugasami Pavadasami, Mohamed Thameem Ansari Musthafa, Vinoth Kumar Natamai Jegananthan, “ Particle swarm optimization Based Dual-Mode Fractional Order Control for Automatic Generation of Two Area Interconnected Hybrid System”, International Journal of Intelligent Engineering and System,Vol.15,No.4,2022.
Srivishnupriya A.P.,Ansari,M.M.T.,&Kumar,N.V, “Automatic generation control of the area hybrid power system by sine cosine optimized dual mode fractional order controller”, International Journal of Renewable Energy Research (IJRER),12(3),1414-1426.
11. N. Singh and A. K. Shukla, “Smart load frequency control with distributed EV chargers,” in Proc. IEEE PES Innovative Smart Grid Technologies, pp. 1–7, 2015.
12. S. Mirjalili, “The Ant Lion Optimizer,” Advances in Engineering Software, vol. 83, pp. 80–98, 2015.
13. B. M. Butun and M. Ayasun, “Design of FOPI controllers using optimization techniques for LFC,” in Proc. IEEE Int. Conf. on Control, Automation and Systems, pp. 125–130, 2018.
14. M. S. Mahmoud and F. M. Al-Sunni, “Adaptive control for LFC of interconnected power systems with electric vehicle integration,” Electric Power Systems Research, vol. 152, pp. 390–399, 2017.
15. Falahati, S., Taher, S. A., & Shahidehpour, M. (2016). A new smart charging method for EVs for frequency control of smart grid. International Journal of Electrical Power & Energy Systems, 83, 458-469.
16. Srivishnupriya A.P., Ansari,M.M.T.,&Kumar,N.V, “Automatic Generation Control of Three Area Hybrid Power System by Sine Cosine Optimized Dual Mode Fractional Order Controller”, International Journal of Renewable Energy Research (IJRER),12(3),1414-1426.
17. R. Ramar, M. Mohamed Thameem Ansari, J. Raja, A.P. Srivishnupriya, “ A Robust Dual Mode Tilt Derivative-Integral Derivative Controller for Frequency Control Considering Renewable Energy Sources and Electrical Vehicle”, International Journal of Renewable Energy Research (IJRER),Vol.15,No.3,September 2025.
18. D.C. Das, A.K Roy, and N. Sinha, “GA based frequency controller for solar thermal–diesel–wind hybrid energy generation/energy storage system”, International Journal of Electrical Power & Energy Systems, Vol.43, No. (1), pp.262-279,2012.
19. M.H. Khooban, T. Niknam, F. Blaabjerg and T. Dragičević, “A new load frequency control strategy for micro-grids with considering electrical vehicles”, Electric Power Systems Research, Vol.143, pp.585-598,2017.
20. M.R.Sathya and M.Mohamed Thameem Ansari, “Design of biogeography optimization based dual mode gain scheduling of fractional order PI load frequency controllers for multi-source interconnected power systems”, International Journal of Electrical Power and Energy Systems, Vol.83, pp.364-381,2016.
21. Sumit kumar,Amit kumar, “A brief review on antlion optimization algorithm”, 2018 International Conference on Advances in Computing, Communication Control and Networking (ICACCCN),12-13,2018.